

The strength of hard-rock pillars

C. D. Martin and W. G. Maybee
School of Engineering, Laurentian University, Canada

Abstract

Observations of pillar failures in Canadian hard rock mines indicate that the dominant mode of failure is progressive slabbing and spalling. Empirical formulas developed for the stability of hard-rock pillars suggest that the pillar strength is not strongly dependent on confining stress. However, stress analyses show that the confinement in a pillar increases significantly beyond a pillar width to height ratio of 0.5.

Two dimensional finite element analyses using conventional Hoek-Brown parameters for typical hard rock pillars (Geological Strength Index of 40, 60 and 80) predicted pillar failure envelopes that did not agree with the observed empirical failure envelopes. It is suggested that the conventional Hoek-Brown failure envelopes over predict the strength of the hard-rock pillars because the failure process is fundamentally controlled by a cohesion-loss process and the frictional strength component can be ignored. Two dimensional elastic analyses were carried out using the Hoek-Brown brittle parameters which only relies on the cohesive strength of the rock mass. The predicted pillar strength curves were generally found to be in agreement with the observed empirical failure envelopes.

1. Introduction

Pillars can be defined as the *in situ* rock between two or more underground openings. Hence, all underground mining methods utilize pillars, either temporary or permanent, to safely extract the ore reserve. In coal mines rectangular pillars are often formed in regular arrays such that should a single pillar fail the load is transferred to adjacent pillars causing these to be over-loaded. This successive overloading process can lead to an unstable progressive "domino" effect whereby large areas of the mine can collapse. This type of failure occurred in 1960 and resulted in the collapse of 900 pillars in the Coalbrook coal mine in South Africa and the loss of 437 lives. Recently, Salamon [1] summarized the extensive research into coal pillar design that followed the Coalbrook disaster. The key element that has been used since 1960 for the successful design of coal pillars is "back-calculation", an approach that has been used extensively in geotechnical engineering[2]. This approach has led to the development of empirical pillar strength formulas but can only be implemented by observing and documenting failed pillars.

The design of hard-rock pillars has not received the same research attention as coal pillar design. In part because fewer mines operate at depths sufficient to induce the stresses required to cause hard rocks to fail, and in hard-rock mining pillar and mining geometries are irregular making it difficult to establish actual loads. Nonetheless as mining depths increase the potential for the failure of hard-rock pillars also increases. This paper focuses on the strength of hard-rock pillars and presents a stability criterion that can be used to

establish hard-rock pillar geometries.

2. Empirical pillar strength formulas

Following the CoalBrook disaster, a major coal-pillar research program was initiated in South Africa. One of the main objectives of this research was to establish the *in situ* strength of coal pillars. Using the back-calculation approach Salamon and Munro [10] analyzed 125 case histories involving coal pillar collapse and proposed that the coal-pillar strength could be adequately determined using the power formula :

$$\sigma_p = K \frac{W^\alpha}{H^\beta} \quad (1)$$

where σ_p is the pillar strength, K is the strength of a unit volume of coal, and W and H are the pillar width and height, respectively. The notion that the strength of a rock mass is to a large part controlled by the geometry of the specimen, i.e. width to height ratio, has since been confirmed by extensive laboratory studies, e.g., [11]. The data from the 125 case studies gave the following values for the parameters in Equation 1: $K = 7.176$ MPa, $\alpha = 0.46$ and $\beta = 0.66$. According to Madden [12] and Salamon [1] Equation 1 has been applied extensively to the design of pillar layouts in South Africa since its introduction in 1967. While it is tempting to apply Equation 1 to other pillar designs, it must be remembered that Equation 1 was developed for room and pillar mining of horizontal coal seams and that the value of K is only typical for South African coal.

One of the earliest investigations into the design of hard-rock pillars was carried out by Hedley and Grant [3]. They

Table 1: Summary of empirical strength formula for hard-rock pillars.

Reference	Pillar strength formulas (MPa)	σ_c (MPa)	Rock mass	No. of pillars
Hedley and Grant [3]	$179 \frac{W^{0.5}}{H^{0.75}}$	230	Quartzites	28
Von Kimmelman et al. [4]	$65 \frac{W^{0.46}}{H^{0.66}}$	94	Metasediments	57
Krauland and Soder [5]	$35.4(0.778 + 0.222 \frac{W}{H})$	100	Limestone	-
Potvin et al. [6]	$0.42 \sigma_c \frac{W}{H}$	-	Canadian Shield	23
Hedley [7]	$133 \frac{W^{0.5}}{H^{0.75}}$	230	Quartzites	28
Sjöberg [8]	$74(0.778 + 0.222 \frac{W}{H})$	240	Limestone/Skarn	9
Lunder and Pakalnis [9]	$0.44 \sigma_c (0.68 + 0.52 \kappa)$	-	Canadian Shield	178

analyzed 28 rib pillars (3 crushed; 2 partially failed and 23 stable) in massive quartzites and conglomerates in the Elliot Lake room and pillar uranium mines. They concluded that the Equation 1 power formula could adequately predict the hard rock pillar failures but that the parameters in Equation 1 needed to be modified to:

$$\sigma_p = K \frac{W^{0.5}}{H^{0.75}} \text{ MPa} \quad (2)$$

The value of K in Equation 2 was initially set as 179 MPa but later reduced to 133 MPa [7].

Since 1972 there have been several additional attempts to establish hard rock pillar strength formulas, using the "back calculation" approach (Table 1). Inspection of Table 1 reveals that either a power or linear formula has been used to predict the pillar strength for a wide range of pillar shapes and rock mass strengths as indicated by the unconfined compressive strength (94 to 240 MPa). Figure 1 shows

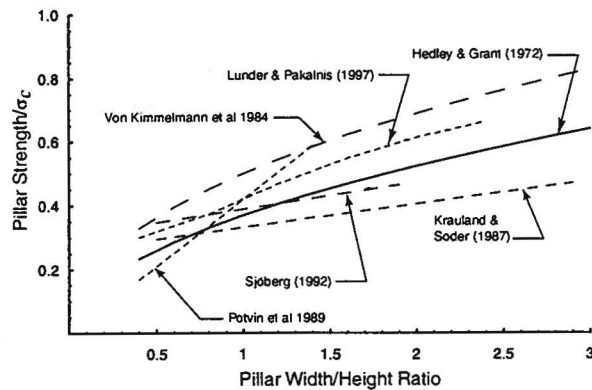


Figure 1: Comparison of the empirical pillar strength formulas in Table 1.

the predicted pillar strength from the various formulas using a constant pillar height of 5 m. The pillar strengths in Figure 1 have been normalized to the laboratory uniaxial compressive strength (σ_c). As shown in Figure 1 the formulas predict very similar strengths, particularly for the pillar width to height ratio between 0.5 and 1.5, the range over which most pillar failures occur.

The stress magnitudes used to establish the pillar strength formulas in Table 1 were determined using either tributary area, or 2- and 3-dimensional elastic analyses and represent either the average maximum pillar stress or the maximum stress at the centre of the pillar. In all cases the pillar-strength formulas ignore the effect of confinement, i.e., σ_3 and rely on a simple stress to strength ratio based on the maximum pillar stress and the uniaxial unconfined compressive strength. This is similar to the stress to strength (σ_1/σ_c) ratio that has been used to predict tunnel stability in South African mines [13].

The elastic stress distribution in pillars is a function of the pillar geometry. These distributions can readily be determined through numerical computer programs. Lunder and Pakalnis [9] examined the stress distribution in hard-rock pillars in Canadian mines and proposed that the average confinement in a pillar could be described by:

$$\frac{\sigma_3}{\sigma_1} = 0.46 \log \left(\frac{W}{H} + 0.75 \right) \left(\frac{1.4}{\frac{W}{H}} \right) \quad (3)$$

where the confinement is expressed as the ratio of σ_3/σ_1 . Figure 2 illustrates Equation 3 and shows that the confinement in pillars increases significantly beyond a pillar width to height ratio of 1. Recently, Maybee [14] showed however, that the rate of increase is a function of K_o , the ratio of the far-field horizontal stress σ_1 and σ_3 (Figure 3). Figure 3 shows that beyond a pillar width to height ratio of 1 the effect of K_o is significant but for pillar width to height ratios less than 1 the effect of K_o can be ignored.

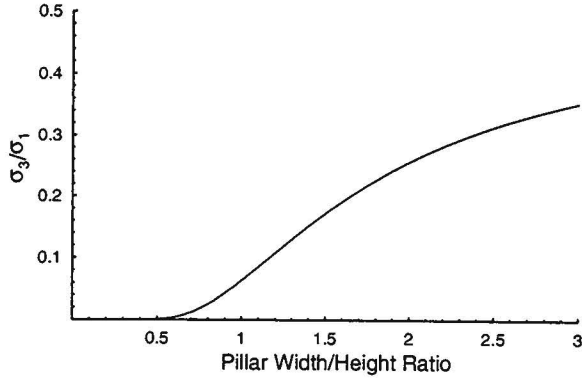


Figure 2: Illustration of the increase in confinement as the pillar width to height ratio increases using Equation 3.

The strength of a rock mass is usually described in terms of a constant cohesive component and a normal-stress or confinement dependent component. Hence for pillars with width to height ratios greater than 1, the strength should increase as the confining stress increases. In the next section the Hoek-Brown failure criterion is used to investigate the effect of confinement on pillar strength.

3. Pillar and rock mass strength

One of the most widely used empirical failure criteria is the Hoek-Brown criterion [13]. Since its introduction in 1980 the criterion has been modified several times, most recently in 1998 [15]. The generalised form of the criterion for jointed rock masses is defined by:

$$\sigma_1 = \sigma_3 + \left(m_b \frac{\sigma_3}{\sigma_{ci}} + s \right)^a \quad (4)$$

where σ_1 and σ_3 are the maximum and minimum effective stresses at failure respectively, m_b is the value of the Hoek-Brown constant m for the rock mass, and s and a are constants which depend upon the characteristics of the rock

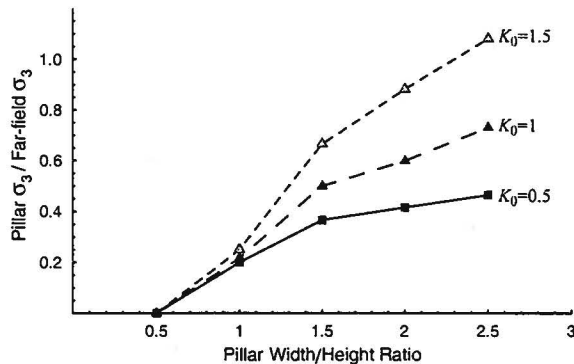


Figure 3: Illustration of the increase in confinement as a function of K_0 , the ratio of the far-field σ_1 and σ_3 .

mass, and σ_{ci} is the uniaxial compressive strength of the intact rock pieces. For hard rock masses, Hoek and Brown [15] recommend a value of 0.5 for a . In order to use the Hoek-Brown criterion for estimating the strength and deformability of jointed rock masses, 'three properties' of the rock mass have to be estimated. These are: (1) uniaxial compressive strength σ_{ci} of the intact rock pieces in the rock mass; (2) Hoek-Brown constant m_i for these intact rock pieces; and (3) Geological Strength Index GSI for the rock mass. The Geological Strength Index was introduced by Hoek and Brown [15] to provide a system for estimating the reduction in the rock mass strength for different geological conditions. The Geological Strength Index can be related to either of the commonly used rock mass classification systems, e.g., the rock mass quality index Q and/or the rock mass rating RMR . Hoek and Brown [15] suggested that GSI can be related to RMR by:

$$GSI = RMR_{39} - 5 \quad (5)$$

where RMR_{39} has the Groundwater rating set to 15 and the Adjustment for Joint Orientation set to zero. The parameters m_b and s can be derived from GSI by the following:

$$m_b = m_i \exp \left(\frac{GSI - 100}{28} \right) \quad (6)$$

$$s = \exp \left(\frac{GSI - 100}{9} \right) \quad (7)$$

The Elliot Lake uranium orebody was actively mined from the early 1950s through to the mid 1990s. The shallow (10 to 15°) dipping tabular deposit was characterized by uranium bearing conglomerates separated by massive quartzite beds 3 to 30 m thick [3, 16]. Mining was carried out using room-and-pillar and stope-and-pillar methods with long (76 m) narrow rib pillars formed in the dip direction. The rock mass Quality of the pillars ranged from Good to Very Good (C. Pritchard, pers. comm.). Seismic surveys carried out across various pillars indicated that at the core of the pillars the P-wave velocity averaged about 6 km/s while at the edge of the pillars the P-wave velocity dropped to 5.5 km/s [16]. Barton and Grimstad [17] proposed the following correlation between seismic compressional wave velocity and rock mass quality Q for non-porous rocks:

$$Q = 10 \frac{V_p - 3500}{1000} \quad (8)$$

This relationship is shown in Figure 4 along with the results from the pillar velocity surveys. These results also support the notion that the pillars were excavated in a Very Good quality rock mass. These descriptions and measurements indicate that the rock mass strength can be characterized by a Geological Strength Index of 80 (Very Good category). This GSI value was used to establish the parameters required for the Hoek-Brown failure criterion (Table 2).

Hoek and Brown [15] suggested that for good quality rock masses the progressive spalling and slabbing nature of the

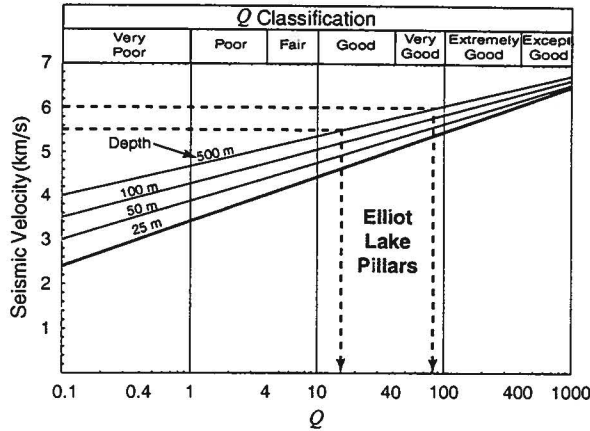


Figure 4: Estimation of the rock mass quality from pillar seismic surveys.

Table 2: Parameters used in the Phase 2 modelling to estimate the strength of the Elliot Lake pillars, assuming an elastic brittle response.

Parameter	Description/Value
Rock Type	Quartzite, Conglomerate
In-situ stress	$\sigma_1 = 2\sigma_3$ and $\sigma_2 = 1.66\sigma_3$ $\sigma_3 = 0.028 \text{ MPa/m}$
Intact rock strength	$\sigma_{ci} = 230 \text{ MPa}$
Geological Strength Index	$GSI = 80$
Hoek-Brown constants	$m_i = 22$ $m_b = 10.7$ $s = 0.108$ $m_r = 1$ $s_r = 0.001$

failure process should be treated in an elastic-brittle manner as shown in Figure 5. This failure process involves significant dilation, and provided there is support to the broken pieces, it is assumed that the failed rock behaves as a cohesionless frictional material. The post-peak Hoek-Brown parameters (m_r, s_r) provided in the Table 2, reflects this assumption.

The original Elliot Lake pillar-database used by Hedley and Grant [3] to establish Equation 2 is shown in Figure 6. Pritchard and Hedley [18] described the progressive spalling and slabbing nature of the failure process of the pillars at these mines and highlighted the difficulty of determining when a pillar has failed. Hedley and Grant [3] classed their pillars as ‘crushed’, ‘partial failure’ and ‘stable’ to reflect the progressive nature of hard-rock pillar failures, and used elastic analyses to determine the loads on the pillars. An example of a ‘crushed’ pillar is given in Figure 7. Hence, the elastic loads for the ‘partial failure’ or ‘crushed’ pillars shown in Figure 6 are not the actual loads because once failure initiates the loads are redistributed either internally within the pillar and/or to adjacent pillars. Numerical analyses were

carried out to determine if the pillar strengths predicted using the Hoek-Brown failure criterion with the parameters in Table 2 were similar to the strength predicted by Equation 2 in Figure 6.

The numerical analyses were carried out using the two di-

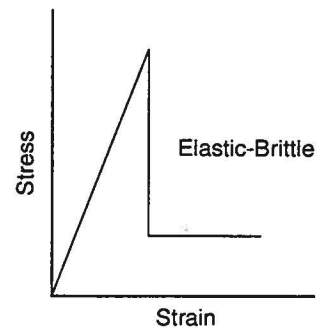


Figure 5: Illustration of the suggested post-failure characteristic for a very good quality hard rock mass.

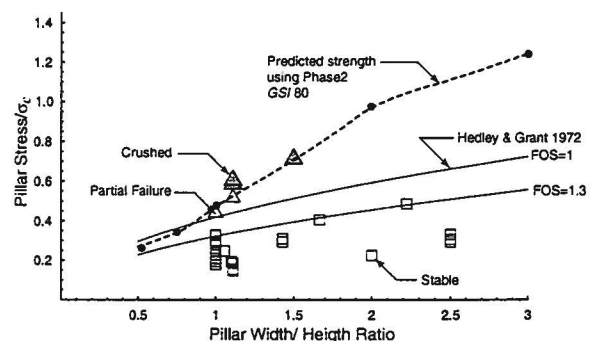


Figure 6: Comparison of the predicted pillar strength using Equation 2 and the observed pillar behaviour in the Elliot Lake uranium mines. Data from Hedley and Grant [3].

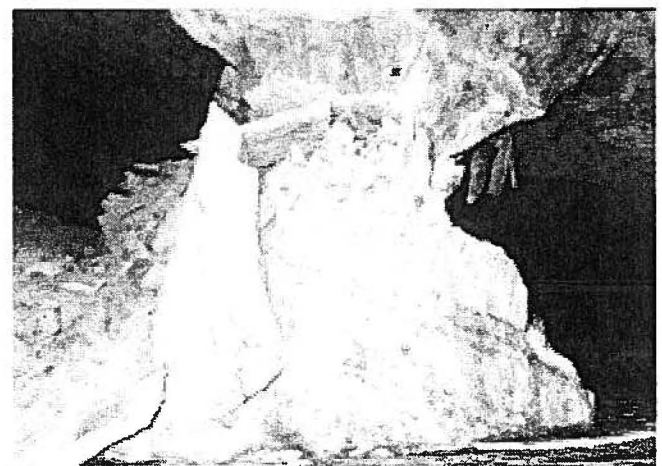


Figure 7: Photo of a ‘crushed’ pillar in massive quartzite.

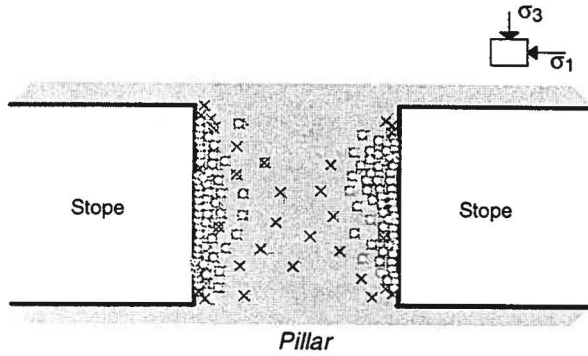


Figure 8: Example of the output from Phase2 showing complete yielding of a pillar with a width to height ratio of 1.

mensional finite element program Phase2¹. This program is very user friendly and has the built in capability to incorporate the elastic-brittle post peak response using the Hoek-Brown parameters. A pillar was considered to have failed when the elements across the pillar had yielded (Figure 8). This was considered similar to the ‘crushed’ conditions in Figure 6. However, in order to compare the stress to strength ratio from the numerical program to the data in Figure 6, the elastic stresses had to be determined for the elastic-brittle failure conditions. These results are presented in Figure 6 and agree with the failed observations for the pillar width to height ratio from 0.5 to 1.5. Beyond a pillar to height ratio of 1.5 the elastic-brittle response appears to over predict the pillar strength compared to Equation 2.

4. Pillar stability criterion and GSI

The Phase2 modelling for the Elliot Lake case study used the Geological Strength Index for a Very Good quality rock mass. In the hard rocks of the Canadian Shield, at the current depths of mining, experience suggests that the Geolog-

¹Available from RocScience Inc. 31 Balsam Ave., Toronto, Ontario, Canada M4E 3B5; Internet:www.rocscience.com

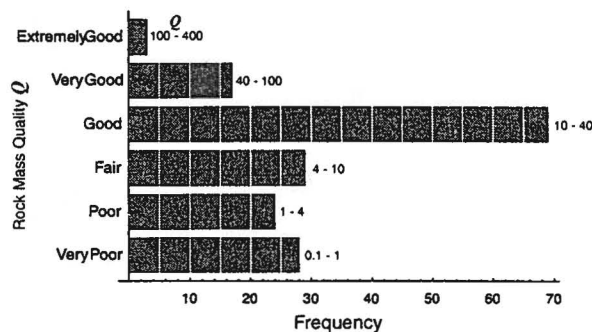


Figure 9: Distribution of the rock mass quality Q in Canadian hard-rock mines, data from Potvin et al. [6].

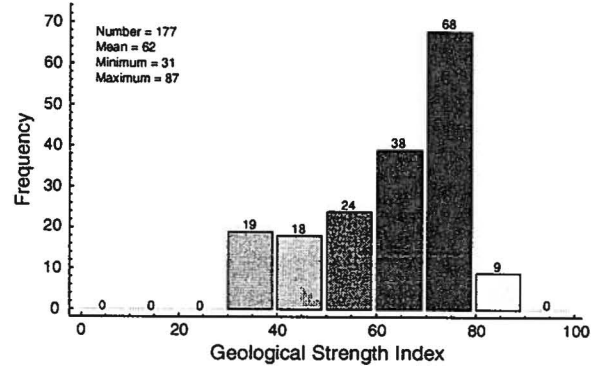


Figure 10: Distribution of the Geological Strength Index (GSI) in Canadian hard-rock mines.

ical Strength Index will vary significantly. Potvin et al. [6] collected 177 case studies from Canadian hard-rock mines and found that Q' defined as:

$$Q' = \frac{RQD}{J_n} \times \frac{J_r}{J_a} \quad (9)$$

where RQD is the Rock Quality Designation
 J_n is the joint set number
 J_r is the joint roughness number
 J_a is the joint alteration number

ranged from 0.1 to 120 (Figure 9). Hoek and Brown [15] suggested that Q' can be used to estimate the value of GSI from:

$$GSI = 9 \ln Q' + 44 \quad (10)$$

The GSI values, using Equation 10 and Potvin et al. [6] database are shown in Figure 10. The GSI values range from 31 (Fair) to 87 (Very Good) with a mean value of 67, suggesting that the GSI values of 40 (Fair), 60 (Good) and 80 (Very Good) would represent the range of typical strength conditions for Canadian hard-rock mines. The corresponding Hoek-Brown parameters for these strength conditions, using Equations 6 and 7, are given in Table 3. Experience suggests that $m_i = 22$ and $\sigma_{ci} = 230$ MPa are typical values for the igneous rocks found in many Canadian hard-rock mines.

The most extensive database of hard-rock pillar failures was compiled by Lunder and Pakalnis [9] who analyzed 140 case histories from mines in the Canadian Shield (Figure 11). Many of these pillars were rib or sill pillars from steeply dipping ore bodies. Lunder and Pakalnis proposed that the pillar strength could be adequately expressed by two factor of safety (FOS) lines. Pillars with a $FOS < 1$ fail while those with a $FOS > 1.4$ are stable. The region between $1 < FOS < 1.4$ is referred to as unstable and pillars in this region are prone to spalling and slabbing but have not completely failed, similar to the ‘partial failure’ used by Hedley and Grant [3]. It should be noted that of the pillars investigated 62 were classed as stable; 39 were classed as failed; and 39 were classed as unstable. For comparison purposes.

the Hedley and Grant pillar strength equation is also shown in Figure 11.

Phase2 numerical analyses were carried out using the same procedure discussed in the Elliot Lake case study to develop pillar stability lines based on the rock mass strength. The Hoek-Brown parameters for *GSI* 40, 60 and 80 given in Table 3 were considered to be representative of the variation of rock mass strength found in Canadian hard-rock mines. The results from this Phase2 modelling are also shown in Figure 11. While the Hedley and Grant pillar strength equation is in good agreement with the stability lines proposed by Lunder and Pakalnis [9], the Phase2 modelling results using the Hoek-Brown failure criterion for *GSI* 40, 60 and 80 do not follow the trends of the stability lines proposed by Hedley and Grant [3] or Lunder and Pakalnis [9]. The general shape of the *GSI* lines reflect the effect of increasing confinement, e.g., see Figures 2 and 3, on the rock mass strength while the observed failure lines appear to be less dependent on confinement. This noticeable trend would suggest that the confining-stress dependent frictional strength component contributes less to the overall pillar strength than the conventional Hoek-Brown failure envelop predicts.

5. Pillar failure and cohesion loss

The failure of hard-rock pillars involves spalling, i.e., slabbing and fracturing, which leads to the progressive deterioration of the pillar strength. Pritchard and Hedley [18] noted that in the early stages of pillar failure at Elliot Lake stress-induced spalling, dominated the failure process while in the latter stages, after spalling had created the typical hour-glass shape, slip along structural features such as bedding planes and joints played a more significant role in the failure process. Martin [19] proposed that this stress-induced spalling/fracturing type failure is fundamentally a cohesion-loss process and Martin et al. [20] suggested that in order to capture this process in numerical models the Hoek-Brown parameters needed to be modified. They proposed that this spalling or brittle type failure could adequately be captured

Table 3: *GSI* and Hoek-Brown strength parameters used in the Phase2 modeling.

	<i>GSI</i>		
	80	60	40
σ_{ci} (MPa)	230	230	230
m_i	22	22	22
m_b	10.77	5.27	2.58
s	0.108	0.0117	0.0013
Residual			
m_r	1	1	1
s_r	0.001	0.001	0.001

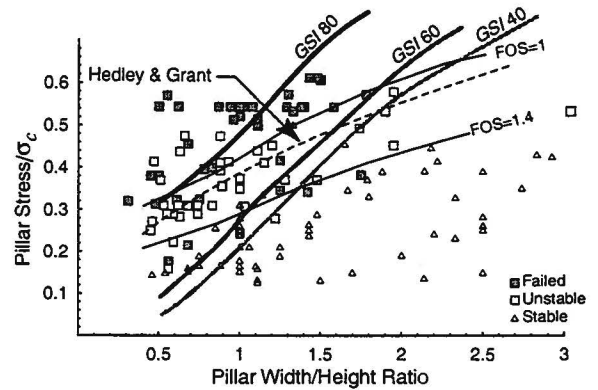


Figure 11: The Pillar Stability Graph developed by Lunder and Pakalnis [9] compared to the pillar strength Equation proposed by Hedley and Grant [3] and the Phase2 modeling results indicated by *GSI* 40, 60 and 80.

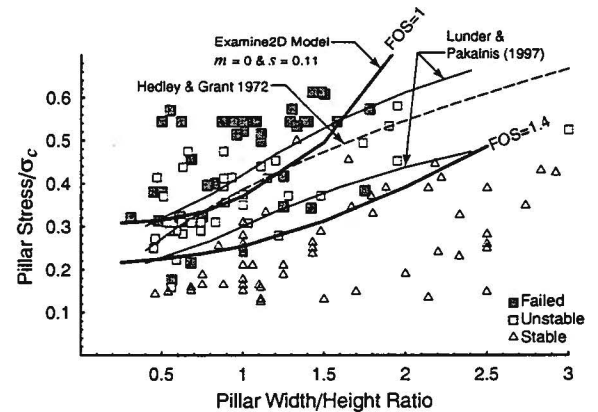


Figure 12: Comparison of the pillar stability graph and the Phase2 modeling results using the Hoek-Brown brittle parameters.

using elastic models and the following Hoek-Brown brittle parameters:

$$m = 0 \text{ and } s = 0.11.$$

The fundamental assumption in using these brittle parameters is that the failure process is dominated by cohesion loss associated with rock mass fracturing and that the confining stress dependent frictional strength component can be ignored. Hence, it is not applicable to conditions where the frictional strength component can be mobilized and dominates the behaviour of the rock mass.

A series of elastic numerical analyses were carried out using the boundary element program Examine2D¹ and the Hoek-Brown brittle parameters to evaluate pillar stability over the range of pillar width to height ratios from 0.5 to 3. The analyses were carried out using a constant K_0 ratio of 1.5 and the results are presented as solid lines in Figure 12 for both a Factor of Safety (*FOS*) equal to 1 and a Factor of Safety equal to 1.4. A pillar was considered to have

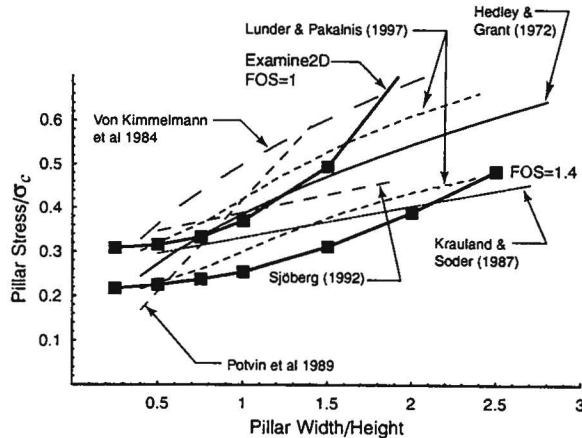


Figure 13: Comparison of hard-rock pillar stability formulae and the Examine2D modeling results using the Hoek-Brown brittle parameters.

failed when the core of the pillar had a $FOS=1$. A similar approach was used to establish when the pillar reached a $FOS=1.4$. Figure 12 shows good agreement between the FOS lines predicted using the Hoek-Brown brittle parameters, and the FOS lines empirically developed by Lunder and Pakalnis [9] and Hedley and Grant [3]. More importantly in contrast to the failure envelopes developed using the Geological Strength Index and the traditional Hoek-Brown parameters (see Figure 11, the slope of the failure envelope using the Hoek-Brown brittle parameters is in closer agreement with the empirical failure envelopes, particularly for pillar width to height ratios from 0.5 to 1.5. Also note that for the pillar width to height ratio less than 1, the strength is essentially constant, reflecting the low confinement for these slender pillars. Beyond a pillar width to height ratio of 2 the numerical results suggest that it is very difficult to get the core of a squat pillar to fail which is also in keeping with practical experience.

Figure 13 shows the comparison of all the empirical formulas listed in Table 1 with the numerical results using the Hoek-Brown brittle parameters. Again, there is good agreement with all the formulas and the predicted results.

6. Conclusions

Observations of pillar failures in Canadian hard rock mines suggest that the dominant mode of failure is progressive slabbing and spalling which eventually leads to an hour-glass shape. The Lunder and Pakalnis pillar stability graph documents over 140 pillar observations in Canadian hard-rock mines and is based on the calculated average maximum stress in the pillar, the unconfined uniaxial strength of the intact rock and the pillar width to height ratio. Their findings are in keeping with other pillar formulas developed for hard-rock pillars and suggest that the pillar strength is not strongly dependent on confining stress, particularly for pillar width to

height ratios less than 1.5, where most pillar failures are observed. However, stress analyses show that the confinement in a pillar increases significantly beyond a pillar width to height ratio of 0.5.

The conventional Hoek-Brown failure envelope is based on a cohesive strength component and a confining stress-dependent frictional component. In a confined state, such as pillar width to height ratios greater than 0.5, the frictional strength component increases significantly. Two dimensional finite element analyses using conventional Hoek-Brown parameters for typical hard rock pillars (Geological Strength Index of 40, 60 and 80) predicted pillar failure envelopes that did not agree with the observed empirical failure envelopes. It is suggested that the conventional Hoek-Brown failure envelopes over predict the strength of the hard-rock pillars because the failure process is fundamentally controlled by a cohesion-loss process and for practical purposes the frictional strength component can be ignored.

Two dimensional elastic analyses were carried out using the Hoek-Brown brittle parameters ($m = 0$, $s = 0.11$). The predicted pillar strength curves were generally found to be in agreement with the observed empirical failure envelopes. It should be noted however, that the Hoek-Brown brittle parameters are not applicable to conditions where the frictional component of the rock mass strength can be mobilized and dominates the behaviour of the rock mass.

Acknowledgements

This work was supported by the Natural Sciences and Engineering Research Council of Canada (NSERC) and through collaboration with the hard rock mining industry in Northern Ontario.

References

1. Salamon M. Strength of coal pillars from back-calculation. In: Amadei B, Kranz RL, Scott GA, Smealie PH, editors, Proc. 37th US Rock Mechanics Symposium, Vail, volume 1. Rotterdam: A. A. Balkema, 1999 29-36.
2. Sakurai S. Back analysis in rock engineering. In: Hudson JA, editor, Comprehensive Rock Engineering - Excavation, Support and Monitoring, volume 4. Oxford: Pergamon Press, 1993 543-569.
3. Hedley DGF, Grant F. Stope-and-pillar design for the Elliot Lake Uranium Mines. Bull Can Inst Min Metall, 1972. 65:37-44.
4. Von Kimmelmann MR, Hyde B, Madgwick RJ. The use of computer applications at BCL Limited in planning pillar extraction and design of mining layouts. In: Brown ET, Hudson JA, editors, Proc. ISRM Symp.: Design and Performance of Underground Excavations. London: British Geotechnical Society, 1984 53-63.

5. Krauland N, Soder PE. Determining pillar strength from pillar failure observations. *Eng Min J*, 1987. 8:34-40.
6. Potvin Y, Hudyma MR, Miller HDS. Design guidelines for open stope support. *Bull Can Min Metall*, 1989. 82:53-62.
7. Hedley DGF. Rockburst handbook for Ontario hardrock mines. CANMET Special Report SP92-1E, Canada Centre for Mineral and Energy Technology, 1992.
8. Sjöberg J. Failure modes and pillar behaviour in the Zinkgruvan mine. In: Tillerson JA, Wawersik WR, editors, Proc. 33rd U.S. Rock Mech. Symp., Sante Fe. Rotterdam: A. A. Balkema, 1992 491-500.
9. Lunder PJ, Pakalnis R. Determination of the strength of hard-rock mine pillars. *Bull Can Inst Min Metall*, 1997. 90:51-55.
10. Salamon MDG, Munro AH. A study of the strength of coal pillars. *J South Afr Inst Min Metall*, 1967. 68:55-67.
11. Hudson JA, Brown ET, Fairhurst C. Shape of the complete stress-strain curve for rock. In: Cording E, editor, Proc. 13th U.S. Symp. on Rock Mechanics, Urbana. New York: American Society of Civil Engineers, 1972 773-795.
12. Madden BJ. A re-assessment of coal-pillar design. *J S African Inst Min and Metall*, 1991. 91:27-36.
13. Hoek E, Brown ET. *Underground Excavations in Rock*. London: The Institution of Mining and Metallurgy, 1980.
14. Maybee WG. Pillar design in hard brittle rocks. Master's thesis. School of Engineering, Laurentian University, Sudbury, ON, Canada, 1999.
15. Hoek E, Brown ET. Practical estimates of rock mass strength. *Int J Rock Mech Min Sci*, 1998. 34:1165-1186.
16. Coates DF, Gyenge M. *Incremental Design in Rock Mechanics*. Monograph 880. Ottawa: Canadian Government Publishing Centre, 1981.
17. Barton N, Grimstad E. The Q-System following twenty years of application in NWT support selection. *Felsbau*, 1994. 12:428-436.
18. Pritchard CJ, Hedley DGF. progressive pillar failure and rockbursting at Denison Mine. In: Young RP, editor, Proc. 3rd Int. Symp. on Rockbursts and Seismicity in Mines, Kingston. Rotterdam: A.A. Balkema, 1993 111-116.
19. Martin CD. Seventeenth Canadian Geotechnical Colloquium: The effect of cohesion loss and stress path on brittle rock strength. *Can Geotech J*, 1997. 34:698-725.
20. Martin CD, Kaiser PK, McCreath DR. Hoek-Brown parameters for predicting the depth of brittle failure around tunnels. *Can Geotech J*, 1999. 36:136-151.